Application of 2D and 3D Electrical Resistivity Tomography (ERT) in Predicting Soil Erodibility in Oredide Village, Auchi in Etsako West LGA of Edo State, Southern Nigeria

[1*]BABAIWA, DA; [2]IKPONMWEN, MO

[1]Department of Science Laboratory Technology, Auchi Polytechnic, Auchi, Nigeria*
[2]Department of Physics, University of Benin, Benin City, Nigeria
Corresponding Author Email: akinbabaiwa@gmail.com, Tel: +234-803-746-9046
Other Author Email: osarogie.ikponmwen@uniben.edu

ABSTRACT: Geoelectrical investigation of the subsurface employing 2D and 3D electrical resistivity tomography (ERT) was carried out to ascertain the soil erodibility in Oredide village, Auchi, Etsako LGA of Edo State with a view to averting imminent colossal damage to land resource and its accompanying infrastructure. A total of 10 traverses, 200 m long each were occupied in grid format using the Dipole - Dipole electrode configuration. 2D results indicate topsoil with resistivity value range of 309 to 40130 Ωm within the depth range of 0 to 5 m. The second layer corresponds to sandy, lateritic sand, sand and sandstone having resistivity values ranging from 2186 to 60350Ωm to a depth of 10.0 m. The third layer has resistivity values indicating lateritic sand, sand and sandstone layer with resistivity values ranging from 2186 to 60350 Ωm within the depth of 20 m. The fourth layer connotes lateritic sand, sand and sandstone to a depth of 30 m. The fifth horizon has resistivity values in the range of 585.2 to 35732.4 Ωm which is representative of sand and sandstone. The maximum depth imaged was 47.7 m. The inverted 2-D resistivity structure shows high resistivity distribution near-surface >1000 Ωm, which are indications of vulnerabilities to erosion in the study area with depth of scouring being 15 m. 3D horizontal depth slice show four layers with depths: 0 – 3.5 m, 3.5– 7.52 m, 7.52 – 12.2 m and 12.2 – 17.5 m having corresponding resistivity values that vary from 465 – 285939 Ωm across each layer respectively. Resistivity values vary from 358 – 217741 Ωm and a 3D depth of 15.4 m was imaged; correlating with the 2D results.

It was Egboka (2000) who defined soil erosion as the steady or sudden removal of sediments (clay, soil, and sand pieces of blocks of minerals) by agents of denudation such as running water (rivers, streams, floods), wind, animals, man, and the resultant transport or removal of weathered sedimentary materials along diverse distances to different and distant locations and ultimate deposition elsewhere. Egboka (2000) sums the causes of erosion into two (2), namely: natural cause, man-made (or anthropogenic) cause. The nature - induced causes are: temperature, nature of soil, earth movement and earth quakes, geology of the earth, climatic conditions which include topography, pressure, rainfall and slope stability problems. Nature of vegetation cover, flowing water, water quality and quantity, physiochemical weathering and other causes of natural mass washing are also agents of erosion. Anthropogenic causes on the other hand, include man in addition to other destructive activities like deforestation. Erosion can also be caused by geological factors such as permeability, porosity and

sediment rock type. The moisture, composition and compaction of soil are all key factors in determining the erosivity of rainfall. Sediments containing more clay appear to be more opposed to erosion when compared with sand or silt, because the clay helps join soil particles together (Nichols, 2009). The land's topography also determines the rate at which surface runoff will flow, which consequently, determines the erosivity of the runoff. Geologic factors generally account for topography while climatic factors alter the efficiency of the erosional processes. Susceptible areas to extreme gully erosion processes, therefore, trace their vulnerability to a combination of distinct geomorphological, geological and pedological characteristics (Ogbonna *et al*., 2011; John *et al.,* 2015).Different methods employed to directly measure erosion rates are expensive and time consuming (Hurst *et al*., 2012) so, causes of erosion are better studied and understood with erosion-prone areas noted for precautionary and remediation actions. It is already established that geologic factor plays critical role in the geomorphology of an area; it

follows that the use of geophysical and geotechnical methods in the evaluation of geologic processes of an area, therefore, comes to play (Uhegbu and John, 2017). Near-surface site characterization employing geophysical methods produces important information connected with the soil characteristics and can also provide a clue into the processes that direct the geomorphic development of landscapes (John *et al.,* 2015; Santamarina *et al*., 2005).Electrical resistivity imaging (ERI)is an intrinsic soil characteristic that denotes a material's ability to resist the passage of current. ER imaging is a near-surface geophysical method to collect bulk continuous ER measurements in relation to a fixed depth. ERI surveys are quick compared with laboratory erosion testing. ER tomography (ERT) is therefore a good method to prioritize scour critical infrastructures premised on predicted soil erodibility. ERT has now been a widely used geophysical technique in fields such as geotechnical engineering, geology, archeology and environmental science (Loke, 1999; Dahlin, 2001; Vaudelet, 2011; Hossain *et al*., 2011; Chambers, 2013 and Snapp, 2017).Additionally, ERT could also be used to quickly identify critical infrastructures such as abutments and bridges having high erosion potential and prioritize scour critical infrastructure monitoring (John *et al*., 2015). Airen and Akeredolu (2020) used 2D and 3D ERI to assess soil erodibility in Uselu quarters, Benin City. Their results revealed that the entire study area is highly vulnerable to erosion as sedimentary subsoil with ERI cutoff above 50 Ωm are classified as highly erodible. It is the aim of this study, therefore, to apply 2D and 3D ERT to probe the erodibility of the subsoil in Oredide village with a view to providing a database of information so that concerned authority can use it for the purpose of curbing the menace.

MATERIALS AND METHODS

Location of the study area: The geophysical survey was carried out in Oredide village with the following coordinates: Latitude 07° 03' 42.2''and Longitude 006° 16' 14.7''. These coordinates were obtained using Garmin 12 Global positioning system (GPS). Actual site observation and information from existing geological maps classify surface sand of the study area and its environs as members of the Ajali formation as presented in Alile, 2008, Babaiwa and Airen**,** 2021.

Data Acquisition: The 2D electrical resistivity study includes the utilization of PASI 16GL model Terrameter resistivity meter which is upheld by an outer battery (12 V, 60 Ah Battery), one Global Positioning System (GPS) for taking the directions of the investigation territory. An aggregate of ten (10) 2D crosses were obtained, as it appears in Figure 2, in a

square grid design utilizing the dipole-dipole exhibit arrangement. This cathode setup was appropriate for steady division information obtaining, so numerous information focuses can be recorded at the same time for every current infusion. Estimations were made at successions of cathodes at n=1, n=2, n=3, n=4 and n=5 cross line utilizing four (4) anodes separated at 10 m apart with between navigate spacing of 50 m from each other and a maximum length of 200 m each.

The 3D electrical resistivity model secured a square grid along the area of investigated zone. The zone was picked to boost inclusion of the focal, northern, and western districts of the researched territory. The overview zone stretches out from 0 to 200 m upper east (y-pivot) and from 0 to 200 m northwest (x-hub) with 10 m electrode separation and between cross dividing of 50 m from one another. The 3D model contains 10 traverse lines, five (5) lines orientated vertically to the x-hub, situated at 10 m spans from 0 to 200 m and five (5) lines orientated on a level plane to the (y-hub), situated at 10 m stretch from 0 to 200 m, separately.

Data Processing: The Dipro software was used for the inversion of the 2D apparent resistivity data. The field data pseudosection and the 2D resistivity structure were produced after running the inversion of the raw data to filter out noise. The Diprofwin program amortizes the bulk data into a series of horizontal and vertical rectangular blocks, with each box containing a number of records. Resistivity of each block was then calculated to produce an apparent resistivity pseudosection. The pseudosection was compared to the actual measurements for a good model fit. The difference between measured and observed values gives the inversion resistivity model which represents the geology of the study area.

The apparent resistivity values for each traverse were collated in a format that is acceptable by the RES3DINV inversion code. Elevation corrections were not included in the measurements as the area surveyed was more or less flat. The entire square set of 2D lines (10 traverses) for each location were merged together to form a single 3D data set each. This was done by collating the measured 2D data (apparent resistivity values) to a 3D data format that can be read by the RES3DINV software. The coordinates, line directions, number of electrodes, electrode spacing and data levels of each of the 2D traverses were used in collating the apparent resistivity values with the aid of an input text file which can be read by the computer code. The collated 3D data sets were inverted using RES3DINVcomputer code which automatically determines a horizontal 3D depth slice model of resistivity distribution using apparent resistivity data

obtained from a 3D resistivity imaging survey (Li and Oldenburg 1992; White *et al*., 2001). Ideally, the electrodes used for such a survey are arranged in square grids. The inversion routine used by the RES3DINV program is based on the smoothness constrained least-squares method. The program allows users to adjust the damping factor and the flatness filters in the equation above to suit the data set being inverted. Initial damping factor of 0.215 was used to invert the collated 3D apparent resistivity data set. After each iterating process, the inversion subroutine generally reduced the damping factor used; a minimum limit (one tenth of the value of the initial damping factor used) was set to stabilize the inversion process. The damping factor was optimized so as to reduce the number of iterations the program requires to converge by finding the optimum damping factor that gives the least RMS error; however, this increases the time taken per iteration. In order to determine the 3D distribution of the model resistivity values from the distribution of apparent resistivity values, the subsurface was subdivided into a number of small square blocks. The program for the first layer thickness based on the maximum depth of investigation of the array was used and was increased by 1.15 (15%) for subsequent layers. Homogeneous earth model was used as the initial model in the inversions carried out. The 3D cube was processed using the Earth Imager 3D by collating the entire square set of 2D lines together to form a single 3D data set each.

RESULTS AND DISCUSSION*Figures completely re numbered. Please check if correct

2D Electrical Resistivity Tomography: The 2D resistivity section along traverse 1 in Oredide is presented in Figure 1. Lateral distance of 200 m was covered and a depth of 30 m is imaged. Resistivity values vary from 5227 – 217741 Ωm across the traverse (Figure 1). Three resistivity structures are delineated which are indications of sand, lateritic sand and sandstone. The resistivity of the sand varies from 5227 – 7911 Ωm and widely distributed along the traverse. The lateritic sand varies in resistivity from 13747 – 18120 Ωm and occurs at lateral distances; 0 – 40 m (from the surface to a depth of 30 m), 70 – 110 m (enclosing a sandstone structure from 5 – 30 m depth) and 110 – 158 m (as a near-surface structure). The sandstone occurs as isolated resistivity structures at lateral distances 80 – 105 m and 120 – 148 m respetively. The high near-surface resistivity values of the resistivity structures are indicative of dry and unconsolidated geologic earth materials which are highly erodible (Karim and Tucker-Kulesza, 2018; Karim *et al*., 2019). The near-surface along this traverse is thus suspected to be prone to deep seated erosion due to deep distributions of the high resistivity values. The sandstone, due to its localized and consolidated nature may be less erodible along the traverse (Figure 1).
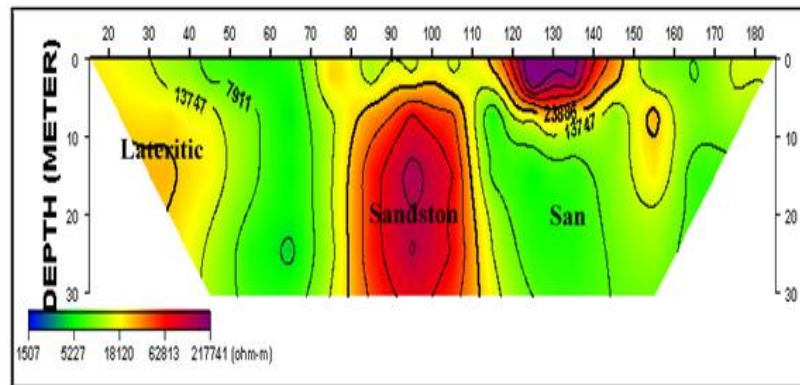
Fig1:2D electrical resistivity section along Oredide, Auchi (Traverse 1)

2-D Resistivity Image along Traverse 10: Figure 3b presents the 2D resistivity section along traverse 10 in Oredide. Horizontal distance of 200 m was covered and a depth of 30 m was imaged. Resistivity values vary from 2186 – 50757 Ωm (Figure 2). Three resistivity structures are delineated which are sand, lateritic sand and sandstone. The sand has resistivity values that vary from 2186 – 6238 Ωm and widely distributed along the traverse from the surface to a depth of 30 m. The lateritic sand has resistivity value of 17794 Ωm and also widely distributed along the traverse from the surface to a depth of 30 m and along the traverse length of 50 – 130 m (Figure 2). The sandstone, having resistivity value of 50757 Ωm occurs at lateral distances; 0 – 50 m, 60 – 95 m and 100 - 130, at corresponding depth range of 0 – 30 m, 5

– 20 m and 0 – 30 m (Figure 2). The traverse is vulnerable to high erodibility whose scouring depth could be as deep as 30 m in some locations and less than 30 m in other locations along the traverse.
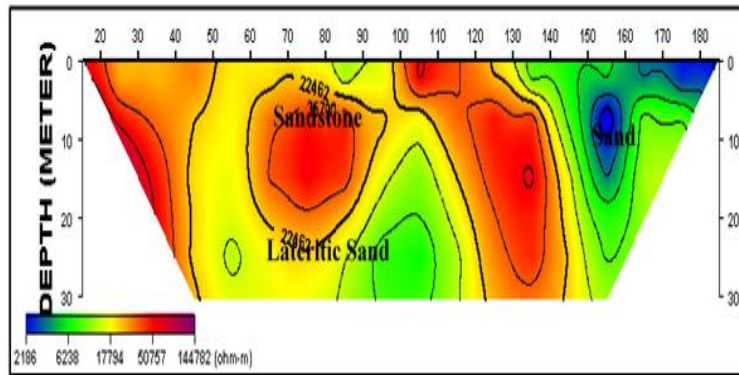
Figure 2: 2D electrical resistivity section along Oredide, Auchi (Traverse 10)

3D Horizontal Depth Slice: Figure 3 shows the 3D horizontal depth slice into four layers across Oredide. The four layers are: 0 – 3.5 m, 3.5– 7.52 m, 7.52 – 12.2 m and 12.2 – 17.5 m with corresponding resistivity values that vary from 465 – 285939 Ωm across each layer respectively (Fig. 3). The slices reveal high resistivity values characterizing the dry and near-surface unconsolidated sand and the sandstone of Ajali Formation (Adekoya *et al.*, 2011; Aleke *et al.*, 2016; Chinyem, 2017; Babaiwa *et al.*, 2020). The high resistivity values may not be unconnected with the fact that soil characteristics like plasticity, water content, grain size, percent clay, compaction, and shear strength which affect soil erosion also influence in-situ bulk soil electrical resistivity (Abu-Hassanein *et al.*, 1996; Grabowski *et al.*, 2011; Kibria and Hossain, 2012; Karim and Tucker-Kulesza, 2017). Soils with electrical resistivity (ER) higher than 50 Ωm have an 87% probability of being classified as highly erodible (Karim and Tucker-Kulesza, 2018; Karim *et al.*, 2019). The depth of erosional impact in Oredide is suspected to be as deep as 12 m. Increased depths in Oredide may be less vulnerable to erosion due to occurrences of consolidated sandstones. Erosional impacts are therefore suspected to decrease with depth in the study area.
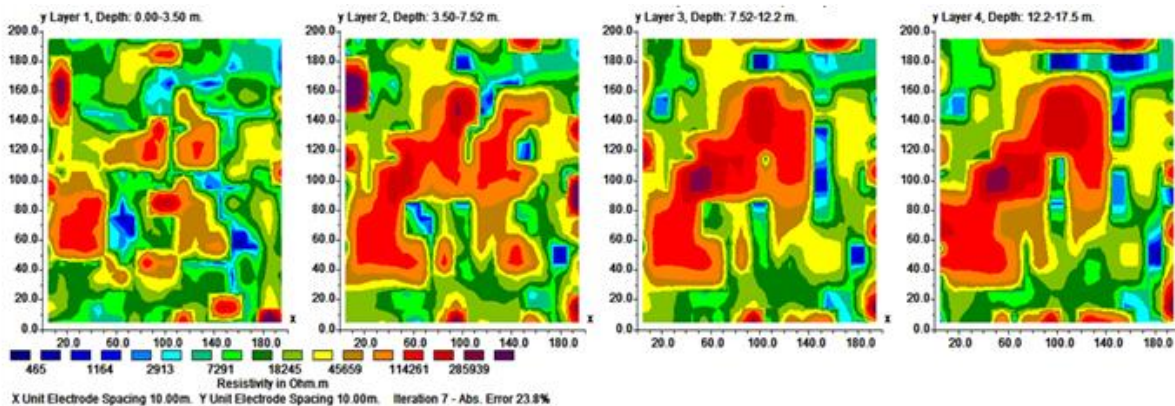
Fig3: Horizontal Depth Slices obtained from the 3D Inversion of Square 2D Profiles in Oredide

3D Electrical Resistivity Modelling: The 3D resistivity block distribution of Oredide is presented in Figure 4 while the 3D apparent resistivity crossplot is presented in Figure 5. Resistivity values vary from 358 – 217741 Ωm and a 3D depth of 15.4 m was imaged. Along the Y-axis of the 3D block compared to X-axes of the resistivity block, where the resistivity varies from 8833 – 217741Ωm and is representative of dry and near-surface unconsolidated sand and the sandstone of Ajali Formation (Adekoya *et al.*, 2011; Aleke *et al.*, 2016; Chinyem, 2017; Babaiwa *et al.*, 2020). The erosional impact is likely to be intense and deep, up to 15 m depth (Fig. 2). Oredide 3D resistivity visualization reveals that the whole area is prone to intense erosional episodes as deep as 12 – 15 m in the area.The apparent resistivity crossplot of Oredide is shown in Figure 5 having an iteration no of 3 and RMS value of 19.8%.
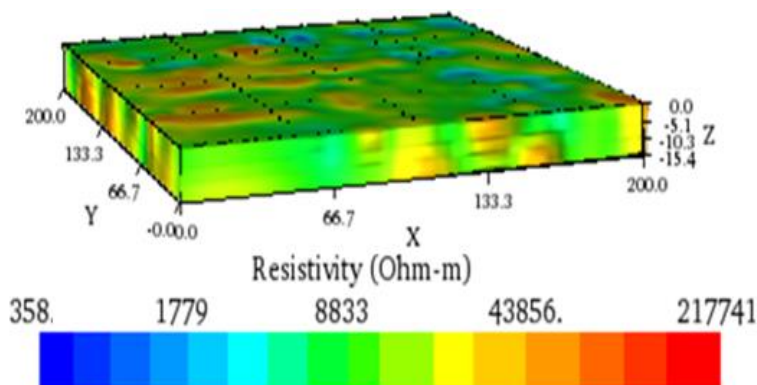
Fig 4:3D resistivity distribution
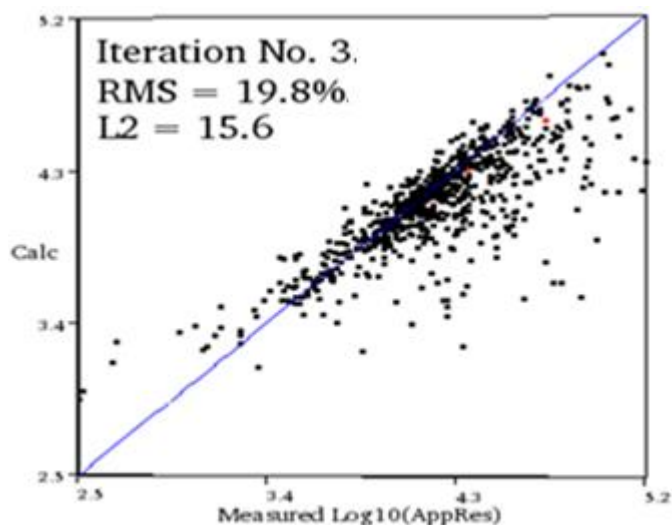
Fig 5: Oredide apparent resistivity crossplot

Conclusion: 2D and 3D electrical resistivity tomography has been used to characterize erosion potential in Oredide village, Auchi in Etsako LGA of Edo State, Nigeria. The 2D results show four geoelectric layers were identified in the study area which is topsoil, lateritic sand, sand and sandstone with resistivity value range of 309 to 40130 Ωm within the depth range of 0 to 5 m. A complementary 3D horizontal depth slice show four layers with depths: 0 – 3.5 m, 3.5 – 7.52 m, 7.52 – 12.2 m and 12.2 – 17.5 m having corresponding resistivity values that varies from 465 – 285939 Ωm across each layer respectively. The slices reveal high resistivity values. Resistivity values vary from 358 – 217741 Ωm and a 3D depth of 15.4 m was imaged. Evidently, the whole area is prone to intense erosional episodes as deep as 12 – 15 m. This study showed that the data obtained from an electrical resistivity survey can predict the presence of highly erosive soils. As such, electrical resistivity surveys may be used to identify where further testing is necessary to measure the scour potential or determine which existing infrastructure should be

protected or closely monitored for scour potential during a flood event.

REFERENCES

Abu-Hassanein, Z; Benson, C; Blotz, L (1996). Electrical resistivity of compacted clays. *J Geotech Eng*; 5(397): 397–406

Adekoya, JA; Aluko, AF; Opeloye, SA (2011). Sedimentological characteristics of Ajali Sandstone in the Benin flank of Anambra Basin, Nigeria. *Ife J. Sci.* 13(2): 327-337

Aleke, CG; Okogbue, CO, Aghamelu, OP; Nnaji, NJ (2016). Hydrogeological potential and qualitative

assessment of groundwater from the Ajali Sandstone at Ninth mile area, southeastern Nigeria. *Environ. Earth Sci.* 75(290): 1-16

Alile, OM., Amadasun, CVO and Evbuomwan, AI (2008). Application of vertical electrical sounding method to decipher the existing subsurface stratification and groundwater occurrence status in a location in Edo North of Nigeria". *Inter. J. Physical Sci.* 3 (10). 245-249.

Airen, OJ and Akeredolu, T (2020). Geophysical assessment of soil erodibility using 2D and 3D electrical resistivity imaging: A case study of Mela Road, Uselu, Benin City, South – South Nigeria. *Australian J. Sci. Tech.* 4. 4

Babaiwa, DA., Aigbogun, CO and Umoru, AT (2020). Aquifer characterization using vertical electrical sounding in Auchi Polytechnic, Auchi, Edo State, Nigeria. *Nig. J.Techn.*39 (3): 925–931.

Babaiwa, DA and Airen, OJ (2021). Characerizing Soil Erosion Potential using Vertical Electrical Sounding (VES) in Oredide Village, Auchi in Etsako West LGA of Edo State, Southern Nigeria (Accepted).

Chambers, JE (2013). River terrace sand and gravel deposit reserve estimation using three-dimensional electrical resistivity tomography for bedrock surface detection. *J Appl. Geophys.*93:25-32.

Chinyem, FI (2017). Evaluation of groundwater potentials for borehole drilling by integrated geophysical mapping of Auchi, South Western Nigeria using very low frequency electromagnetic profiling (VLF-EM) and vertical electrical sounding (VES). *J. Appl. Sci. Environ. Manage.* 21(4): 693-700

Dahlin, T (2001). The development of DC resistivity imaging techniques. *Compute. Geosci.* 27:1019-29.

Egboka BC (2000). Erosion, Its Causes and Remedies. A Key Note Address on Erosion Control and Sustainable Environment. University of Nigeria, Nsukka, Nigeria

Grabowski, RC; Droppo, IG and Wharton, G (2011). Erodibility of cohesive sediment: The importance of sediment properties. *Earth Sci. Rev.* 105(3): 101–120

Hossain, MS; Khan, MS, Hossain, J, Kibria, G, Taufiq, T (2011). Evaluation of unknown foundation depth using different NDT methods. *J Geotech. Geoenviron. Eng.* 27:209-14.

Hurst, MD; Mudd, SM, Walcott, R, Attal, M and Yoo K (2012). Using hilltop curvature to derive the spatial distribution of erosion rates. *J Geophys Res*; 117. DOI: 10.1029/2011JF002057.

John, UJ, Igboekwe, MU and Amos-Uhegbu, C (2015). Geophysical evaluation of erosion sites in some parts of Abia state, Southeastern Nigeria. *Phys. Sci. Int. J,* 6:66-81.

Karim, MZ and Tucker-Kulesza, SE (2017). Two-dimensional soil erosion profile using electrical resistivity surveys. *Geotech Frontiers*; ASCE, Reston, VA

Karim, MZ and Tucker-Kulesza, SE (2018). Predicting soil erodibility using electrical resistivity tomography. *J. Geotech Geoenviron. Eng.* 144(4):04018012.

Karima, MZ, Tucker-Kuleszaa, SE and Bernhardt-Barry, M (2019). Electrical resistivity as a binary classifier for bridge scour evaluation. *Trans Geotech*; 19:146-157

Kibria, G and Hossain, MS (2012). Investigation of geotechnical parameters affecting electrical resistivity of compacted clays. *J Geotech Geoenviron. Eng.* 10:1520–1529

Li, Y and Oldenburg, DW (1992). Approximate inverse mappings in DC resistivity problems. *Geophysical J. Inter.* 109, 343-362.

Loke, MH (1999). Electrical Imaging Surveys for Environmental and Engineering Studies 2017.Availablefrom:http://www.moho.ess.ucla.edu/?pdavis/ess135_2013/literature/%20lokedcresistivity.pdf. [Last accessed on 2017 Feb 22].

Nichols, G (2009). Sedimentology and Stratigraphy. New York: John Wiley & Sons; 93.

Ogbonna, JU; Alozie, M, Nkemdirim, V and Eze, MU (2011). GIS analysis for mapping gully erosion impacts on the geo-formation of the Old Imo State, Nigeria. *ABSU J Environ Sci. Technol.* 1:48-61.

Santamarina, JC; Rinaldi, VA, Fratta, D, Klein, KA, Wang, YH, Cho GC, *et al*., (2005) Survey of

elastic and electromagnetic properties of near surface soils. In: Near Surface Geophysics. Investigation in Geophysics, No. 13.

Snapp, M, Tucker-Kulesza, S, Koehn, W (2017). Electrical resistivity of mechanically stabilized earth wall backfill. *J Appl. Geophys,* 141:98-106.

Uhegbu, CA, and John, UJ (2017). Geophysical and geotechnical evaluation of erosion sites in Ebem-Ohafia area of Abia state, Southern Nigeria. *Adv Res*; 10:1-14.

Vaudelet, P (2011). Mapping of contaminant plumes with geoelectrical methods. A case study in urban context. *J. Appl. Geophys.* 75:738-751.

White, RMS; Collins, S, Denne, R, Hee, R and Brown, P (2001). A new survey design for 3D IP modelling at Copper hill. *Exploration Geophysics.* 32, 152-155